HHS Public Access

Author manuscript

J Neurosurg. Author manuscript; available in PMC 2016 January 11.

Published in final edited form as:

J Neurosurg. 2014 April ; 120(4): 988–996. doi:10.3171/2013.12.JNS131537.

Fiber tractography of the axonal pathways linking the basal ganglia and cerebellum in Parkinson disease: implications for targeting in deep brain stimulation

Jennifer A. Sweet, M.D.[1], **Benjamin L. Walter, M.D.**[2], **Kabilar Gunalan, M.S.**[3], **Ashutosh Chaturvedi, Ph.D.**[3], **Cameron C. Mcintyre, Ph.D.**[3], and **Jonathan P. Miller, M.D.**[1]

[1]Department of Neurosurgery, The Neurological Institute, University Hospitals Case Medical Center, Cleveland [2]Department of Neurology, The Neurological Institute, University Hospitals Case Medical Center, Cleveland [3]Department of Biomedical Engineering, Case Western Reserve University, Cleveland, Ohio

Abstract

Object—Stimulation of white matter pathways near targeted structures may contribute to therapeutic effects of deep brain stimulation (DBS) for patients with Parkinson disease (PD). Two tracts linking the basal ganglia and cerebellum have been described in primates: the subthalamopontocerebellar tract (SPCT) and the dentatothalamic tract (DTT). The authors used fiber tractography to evaluate white matter tracts that connect the cerebellum to the region of the basal ganglia in patients with PD who were candidates for DBS.

Methods—Fourteen patients with advanced PD underwent 3-T MRI, including 30-directional diffusion-weighted imaging sequences. Diffusion tensor tractography was performed using 2 regions of interest: ipsilateral subthalamic and red nuclei, and contralateral cerebellar hemisphere. Nine patients underwent subthalamic DBS, and the course of each tract was observed relative to the location of the most effective stimulation contact and the volume of tissue activated.

Results—In all patients 2 distinct tracts were identified that corresponded closely to the described anatomical features of the SPCT and DTT, respectively. The mean overall distance from the active contact to the DTT was 2.18 ± 0.35 mm, and the mean proportional distance relative to the volume of tissue activated was 1.35 ± 0.48. There was a nonsignificant trend toward better postoperative tremor control in patients with electrodes closer to the DTT.

Address correspondence to: Jonathan P. Miller, M.D., 11100 Euclid Ave., Cleveland, OH 44106. jonathan.miller@uhhospitals.org.

Disclosure: Dr. McIntyre is a consultant for Boston Scientific Neuromodulation Corp., and has an ownership interest in Surgical Information Sciences, Inc. The other authors have no sources of financial and material support to disclose, and they report no conflict of interest concerning the materials or methods used in this study or the findings specified in this paper.

Author contributions to the study and manuscript preparation include the following. Conception and design: all authors. Acquisition of data: all authors. Analysis and interpretation of data: all authors. Drafting the article: Sweet, Walter, Gunalan, Chaturvedi, McIntyre. Critically revising the article: all authors. Reviewed submitted version of manuscript: all authors. Approved the final version of the manuscript on behalf of all authors: Miller. Statistical analysis: Miller, Sweet, Walter, Gunalan. Administrative/technical/material support: Miller, Sweet, Walter, Gunalan.

Conclusions—The SPCT and the DTT may be related to the expression of symptoms in PD, and this may have implications for DBS targeting. The use of tractography to identify the DTT might assist with DBS targeting in the future.

Keywords

deep brain stimulation; diffusion tensor imaging; fiber tractography; Parkinson disease; tremor; functional neurosurgery

The optimal surgical target for deep brain stimulation (DBS) in patients with medically refractory Parkinson disease (PD) remains a subject of debate. Although the safety and efficacy of subthalamic and pallidal stimulation to control PD symptoms has been well demonstrated,[8,16] it is postulated that much of the benefit achieved from DBS is due to indirect stimulation of white matter pathways traveling in close proximity to the active contact of the stimulating electrode.[11,17,20] In spite of technological improvements in diffusion-weighted imaging (DWI), targeting of white matter tracts has yet to be implemented in clinical practice. Nevertheless, given the complexity of the networks and fiber pathways involved in the pathogenesis of PD, it is likely that a better understanding of the structures targeted would lead to improved outcome.

Although abnormal activity within the basal ganglia has long been associated with the pathophysiological findings of PD, the role of the cerebellum is less clear. Alterations in function of the cerebellum and basal ganglia have been documented in patients with PD, and these changes have been shown to normalize after successful treatment with DBS.[9,23] Recent retrograde transneuronal viral transport labeling studies in nonhuman primates have revealed 2 consistent tracts that link the basal ganglia and cerebellum and that may be involved in clinical manifestations of PD.[2,12] The descending subthalamopontocerebellar tract (SPCT) projects from the subthalamic nucleus (STN) to the pons, traverses the superior cerebellar peduncle, and terminates in the cerebellar cortex.[3] The ascending dentatothalamic tract (DTT) projects medially from the dentate nucleus through the superior cerebellar peduncle to the intralaminar thalamic nuclei as well as the ventral anterior, ventral lateral, centromedian, and centrolateral nuclei of the thalamus, and has projections into motor regions of the putamen.[12] These tracts have not been extensively characterized in humans and their relationship to classic DBS targets is not known.

In this study we used DWI-based fiber tractography to identify and characterize both of the previously described white matter tracts that connect the basal ganglia and cerebellum in patients with PD. Additionally, in patients in whom STN electrodes had been implanted, we evaluated the relationship of these tracts to the active contact by using direct measurement and evaluation of the volume of tissue activated (VTA) to gain a better understanding of neural networks involved in PD and the mechanism of action of DBS.

Methods

Patient Selection

The study was approved by the University Hospitals Case Medical Center Institutional Review Board. Fourteen patients with medically intractable idiopathic PD were included in

the study. All patients underwent MRI between November 2011 and August 2012. Prior to surgery, all patients passed neuropsychological testing that established their surgical candidacy, and all exhibited at least 30% improvement of symptoms with levodopa on-off testing as measured by the Unified Parkinson's Disease Rating Scale (UPDRS) Part III.[6,18]

Imaging Protocols

All patients underwent prospective MRI examinations in which a 3-T MRI scanner (Siemens) equipped with 8 receiver channels and fast gradients was used. Sequences obtained for preoperative surgical targeting included 3D T1-weighted, post-Gd MRI as a reference data set (number of slices 160, flip angle 9°, slice thickness 1 mm, pixel size 0.67 × 0.67, TR 1600 msec, TE 3.05 msec); 3D T2-weighted FLAIR images (number of slices 160, flip angle 120°, slice thickness 1 mm, pixel size 0.5 × 0.5, TR 6000 msec, TE 356 msec); and modified 3D Tl-weighted fast gray matter acquisition T1 inversion recovery ([FGATIR] ref) (number of slices 160, flip angle 9°, slice thickness 1 mm, pixel size 0.8 × 0.8, TR 3000 msec, TE 3.01 msec). The DWI sequences were also obtained on a 3-T MRI unit (Siemens) with 8 receiver channels and sensitivity encoding (SENSE, Siemens) echo planar imaging with pulse sequence (number of slices 72, flip angle 90°, slice thickness 1.8 mm, matrix 128 × 128, gradient directions 30, b values 0 and 1000 sec/mm^2, TR 11,600 msec, TE 99 msec). In patients who underwent surgery, we obtained a volumetric CT scan of the head (Brilliance iCT, 256-slice, Philips) in a Leksell frame on the day of surgery (number of slices 232, slice thickness 1 mm) and a volumetric CT scan on postoperative Day 1 to evaluate the electrode position (number of slices 232, slice thickness 1 mm).

Surgical Procedure

In a subset of 9 patients, DBS electrodes were placed unilaterally (n = 2) or bilaterally (n = 7) in the STN as described previously.[16] Targeting was performed using iPlan Stereotaxy 3.0 imaging software (BrainLab). An initial indirect target was used of x = ± 12 mm, y = −4 mm, and z = −4 mm relative to the midcommissural point, and was modified using volumetric FLAIR imaging to target the dorsal STN. Intraoperative microelectrode recording was performed to confirm and refine the location of the electrode contacts within the STN, and intraoperative stimulation was performed to verify clinical benefit without side effects. A Medtronic 3389 DBS electrode was implanted and connected to an Activa PC (or SC) implanted neurostimulator in a separate operation.

Postprocessing Protocol

Imaging data were transferred to a neuronavigation workstation (iPlan Stereotaxy 3.0) for postacquisition processing. Using the iPlan Automatic Imaging Fusion software (BrainLab), the diffusion tensor imaging, MRI, and CT (if applicable) sequences were fused to generate 3D surface-rendered reconstruction models. The iPlan FiberTracking software (BrainLab) was used to perform deterministic fiber tractography between specified regions of interest (ROIs). Two ROIs were created based on anatomical landmarks as visualized on the volumetric FLAIR sequences by using iPlan imaging software. ROI 1 was defined as using a cubic box that surrounded the ipsilateral STN and red nucleus together in the anterior mesencephalon, both of which were manually contoured using the BrainLab imaging software. Similarly, ROI 2 was delineated as a cubic box within the contralateral cerebellar

hemisphere excluding the cerebellar peduncles and brainstem (Fig. 1), and the dentate nucleus was also manually contoured. Diffusion tensor tractography was used to visualize fibers tracts traversing both ROIs. The fractional anisotropy threshold was 0.14, and the minimum fiber length was 14 mm.

After performing tractography bilaterally for all patients, tract morphological features were evaluated using iPlan software. For the subset of 9 individuals who underwent DBS of the STN, the relevant nuclei were contoured (Fig. 2), as was the active contact on each electrode as determined from postoperative programming sessions (Fig. 3A). The active contact was defined as the cathodal electrode for either monopolar or bipolar stimulation. The proximity of the active contact to each of the isolated fiber tracts was measured as the point of closest approach. The euclidean distance from the active contact to the closest point of approach of each tract in the x, y, and z axes was calculated using the following formula: distance = v (x^2 + y^2 + z^2). The VTA was calculated from each patient's specific stimulation parameter settings (Fig. 3B).[4] A custom Python-based program using Python libraries (Enthought Python Distribution) was used for visualization. The proximity of the fiber tract to the active contact relative to the VTA was characterized as a proportional distance to the edge of the VTA. This value is defined as $x^2/a^2 + y^2/b^2 + z^2/c^2$, where a, b, and c are the major axes of the VTA ellipsoid in the x, y, and z directions, respectively. Therefore, a point lying exactly on the outer border of the VTA will have a proximity score of 1.0. Lower values will indicate points closer to the active contact, with the number proportional to the distance relative to the shape of the VTA in all 3 dimensions.

Clinical Data Collection

The clinical charts of all patients were reviewed. Demographic information including sex, age, handedness, predominant symptoms according to the UPDRS III, side of predominant symptoms, and side of predominant tremor, if present, were recorded. The predominant symptoms were determined based on the UPDRS III subscores for tremor, bradykinesia, and rigidity. The tremor subscore was calculated by adding together the midline head tremor score with the tremor score for each limb, and then dividing by 3. The tremor score for each limb included the sum of the resting and active tremor scores for that side. Similarly, the rigidity subscore was determined by adding the midline neck rigidity score to the rigidity score for each limb and then dividing by 3. The bradykinesia subscore added together 2 midline values along with the bradykinesia limb score for each side and then divided by 4. The 2 midline bradykinesia components included body bradykinesia and gait, while limb bradykinesia included finger tapping and leg agility. In this way, each of the 3 primary motor symptoms evaluated (tremor, rigidity, and bradykinesia) were believed to be equally weighted. Of the patients who underwent surgery, postoperative electrode programming sessions were used to assess program settings and to determine the active electrode contacts.

Statistical Analysis

Statistical analysis was performed using the Statistical Toolbox in Microsoft Excel 2003. One-way ANOVA was used for parametric data, with $p < 0.05$ considered statistically significant.

Results

Patient Data

Eight men and 6 women were included. The mean age at imaging was 70.5 years (range 49–78 years). All patients had symptoms of rigidity and bradykinesia. Eleven patients (79%) presented with tremor, 5 of whom (45%) had tremor-predominant symptoms. Patients underwent dopaminergic on-off response testing, with improvement ranging from 15%–65% (Table 1). At the time of analysis, 9 of the patients (5 men and 4 women) had undergone implantation and programming of the DBS system. A summary of the programming settings and lead location can be found in Tables 2 and 3, respectively. All patients with tremor had improvement of their tremor, and values for the pre- and postoperative tremor, bradykinesia, and rigidity subscores are listed in Table 4.

Tract Morphology

In all 14 patients, 2 distinct tracts were identified on both sides corresponding to the previously described course of the SPCT and DTT (Fig. 4). Both tracts were occasionally seen to have 2 distinct paths (26% of SPCT and 20% of DTT), but the points of origin and termination and the anatomical course were similar.

In each patient, the SPCT was observed to originate in the STN and descend through the brainstem and decussate in the pons. The decussation occurred in the upper pons near the pontomesencephalic junction in 25 (64%) of 39 tracts (including duplicates), and in the mid pons in 14 (36%) of 39 tracts. Twenty-one (54%) of 39 tracts were noted to make a sharp turn prior to decussation. After crossing the midline, each tract seen was observed to enter the lateral superior cerebellar peduncle and travel to the dorsal surface of the contralateral cerebellar hemisphere in the inferior semilunar lobule.

The DTT was seen to originate in the dentate nucleus of the cerebellum, ascend adjacent to the fourth ventricle, traverse the superior cerebellar peduncle, ascend in the brainstem medially, and decussate in the mesencephalon. The decussation occurred at the level of the red nucleus in 20 (57%) of 35 tracts (including duplicates) and below the red nucleus in 15 (43%) of 35 tracts. Twenty (57%) of 35 tracts were noted to make a sharp turn prior to decussation. After crossing midline, the tract was noted to travel through the red nucleus and traverse the ventrolateral thalamus in all patients (which was confirmed using stereotactic coordinates localizing this region of the thalamus), and then to travel to the striatum.

Location of Active Contact

Sixteen electrodes were implanted in 9 patients. The mean overall distance from the active contact to the nearest approach of the tract was 2.18 ± 0.35 mm, and the mean proportional distance relative to the VTA was 1.35 ± 0.48.

No significant relationship was observed between outcome and actual or VTA-proportional distance from the active contact to the DTT ($F[2,13] = 1.037$, $p = 0.382$). However, a nonsignificant trend toward better outcome when the active contact was closer to the DTT was more clear when the VTA-proportional distance was used (Fig. 5).

Discussion

This study has 2 principal findings. First, we identified 2 white matter tracts in humans that had been previously described in nonhuman primates, the SPCT and DTT, which link the basal ganglia to the cerebellum. Second, we found that the most effective contact in the patients with implanted electrodes was close to the DTT. We also found that the distance from the active contact to the DTT might influence tremor outcome, although this did not reach statistical significance. These findings challenge the traditional paradigm in which the thalamocortical axis is influenced by 2 independent circuits: the basal ganglia (as originally described by Albin and DeLong and as discussed in a later work by Walter and Vitek),[22] and the cerebellum, with no direct connections between either circuit.[14]

In contrast, our data support the findings of Hoshi and colleagues[12] and Bostan and colleagues,[2] suggesting that distinct anatomical connections link the basal ganglia to the cerebellum, because we found that the DTT originates in the dentate, traverses the contralateral red nucleus and ventrolateral thalamus, and then travels to the striatum, whereas the SPCT originates in the STN and travels to the contralateral cerebellar hemisphere. Moreover, these tracts may play a role in the symptomatology of PD because the contact that is most efficacious in relieving symptoms frequently lies within close proximity to the DTT and is often included within the VTA. Although neither achieved statistical significance, we found a more robust trend toward correlation with outcome when VTA-proportional distance rather than actual distance was considered, which might indicate that VTA is a more clinically meaningful measure of tract activation.

Parkinson Disease and Tremor

The symptoms of rigidity and bradykinesia seen in patients with PD are thought to result from dopaminergic neuronal degeneration, with downstream effects in the basal ganglia. However, the cause of resting tremor, with which more than half of all PD patients present, is unclear.[7,13] Although metabolic imaging studies performed using PET and SPECT show a strong correlation between decreased dopamine synthesis and the presence of bradykinesia and rigidity, this relationship is much weaker with regard to resting tremor.[7] Likewise, drug treatment studies in patients with PD who have levodopa-refractory tremor show improvement of tremor with the addition of drugs such as dopamine agonists, anticholinergics, atypical neuroleptics, and glutamate antagonists. None of these agents, though, are as effective as levodopa for controlling patient rigidity and bradykinesia.[7] Thus, the loss of dopaminergic function within the basal ganglia may not be the only system involved in the pathogenesis of PD, and the connection between the basal ganglia and the thalamocortical axis may not exist in isolation.

Parkinson Disease and the Cerebellum

Investigators have explored the nature of tremor in patients with PD and the role of the cerebellum in this process. In patients with PD, tremor-related oscillatory activity has been recorded in the STN, in the internal globus pallidus, and in the ventral intermediate nucleus of the thalamus.[1,13,15] Lesioning or stimulation of the ventral intermediate thalamic nucleus, which receives input from the cerebellum, has proven to be extremely efficacious in treating

parkinsonian tremor.[3,15] By contrast, the ventral anterior and ventral oral posterior thalamic nuclei have not been found to have such oscillatory activity in spite of robust input from the internal globus pallidus, and these regions have not been shown to be effective targets when stimulated for the treatment of tremor.[2,3,10,15,19] Thus, although the basal ganglia and the cerebellum target distinctly separate regions of the thalamus with their projection fibers, tremor-related oscillations are found in the basal ganglia and in the cerebellar-associated thalamus.

In studies that assess brain activity in patients with PD, the cerebellum has consistently been found to be overactive during motor-related tasks when compared with healthy subjects.[21,23,24] One such study in which functional MRI was used during repetitive motor activities found hyperactivity in the cerebellum that was thought to be a compensatory mechanism to counteract the abnormal function of the basal ganglia.[23] In another study, patients with PD in whom DBS electrodes had been implanted in the STN performed dual-motor tasks during PET studies while receiving either subtherapeutic or therapeutic STN stimulation. Increased metabolism in the cerebellum was observed to normalize in patients who received therapeutic stimulation.[9] These reports support the notion that the cerebellum may affect the motor manifestations of PD.

If the cerebellum is directly involved in the pathogenesis of PD, white matter pathways connecting the cerebellum to the basal ganglia are likely to be involved. Two such tracts have been identified: the DTT and the SPCT. The DTT was discovered by Hoshi and colleagues,[12] who in 2005 injected rabies virus into the sensorimotor area of the putamen of nonhuman primates to trace the site of neuronal projections innervating the injected target. The synapses from the retrograde transneuronal virus were followed, and the first-order neurons were found to be in the ventrolateral thalamus. Second-order neurons that projected to the ventrolateral thalamus were found to be in the contralateral dentate nucleus of the cerebellum. Thus, the authors demonstrated a clear, disynaptic pathway connecting the output center of the cerebellum (the dentate nucleus) to the input center of the basal ganglia (the striatum). In the second part of their study, the authors injected the virus into the external globus pallidus and again followed its synapses to find first-order neurons in the striatum; second-order neurons in the intralaminar nuclei, ventroanterior, and ventrolateral thalamus; and third-order neurons in the dentate. From this exercise they realized that the cerebellum not only innervates the striatum via the DTT but goes on to affect the external globus pallidus, which is involved in the indirect pathway of the circuitry of the basal ganglia.[12]

In a follow-up study, in 2010 Bostan and colleagues[2] injected the rabies virus into the cerebellar cortex of non-human primates. Using similar methodology, they traced the retrograde, transneuronal, viral synapses to the site of original neuronal projections. The authors found that the first-order neurons, which directly innervated the cerebellar cortex, arose from the pontine nuclei, and the second-order neurons that innervated the first-order neurons came from the STN. Bostan and colleagues concluded that another independent, disynaptic connection existed between the basal ganglia and the cerebellum. This tract began in the STN, descended in the brainstem toward the pons, and made its first synapse in the pontine nuclei. The fibers then decussated in the pons and entered the contralateral

cerebellar cortex via the superior cerebellar peduncle. The results from Bostan and colleagues show that that not only is there an independent, disynaptic connection from the dentate nucleus of the cerebellum to the striatum, but there is also a reciprocal independent, disynaptic pathway from the STN to the cerebellum.[3]

Clinical Implications

The DTT has been identified in a previous report using DWI and fiber tracking in a single patient with tremor-predominant PD who underwent implantation with a unilateral ventral intermediate thalamic electrode.[5] Deterministic tractography demonstrated a close anatomical relationship between the active DBS electrode contact and the DTT. In our report on 14 patients with PD, of whom 9 received implants with STN DBS electrodes, we similarly found that the DTT was within close proximity to the active contact. Furthermore, the DTT was frequently (75%) within the VTA, suggesting that stimulation of the DTT may be responsible for symptom relief in patients with PD.

Study Limitations

Limitations of this study include the small patient population, precluding determination of statistical significance, and the heterogeneity of the study population given that not all of the patients underwent DBS surgery and that only a subset of patients were tremor predominant. Further investigations are necessary with a larger population of patients with tremor-predominant PD for an accurate evaluation of the location of the active electrode contact relative to these tracts. With a larger number of patients, one might also be able to better assess the relationship between the rigidity and bradykinesia motor symptoms and either the DTT or perhaps even the SPCT. Comparison with a healthy control group and with patients suffering from other movement disorders, such as essential tremor, might provide additional information.

As mentioned in the foregoing discussion, some evidence suggests that alterations in cerebellar function in PD arise as a secondary, compensatory mechanism to counteract the abnormal basal ganglia circuitry seen in PD.[23] Thus, it is possible that the correlation between the DTT and tremor symptoms suggested in the current study may represent an epiphenomenon rather than a primary association. Future investigations assessing white matter tract involvement in patients with tremor-predominant PD compared with patients with essential tremor, which is thought to result from a primary derangement of cerebellar function, may provide further insight into the pathophysiological mechanisms of the tremor component of PD.

Another limitation of the study involves the inherent limitations of fiber tracking algorithms, which may produce errors wherever fibers cross. Moreover, because the ROI used in the study included the cerebellar hemisphere rather than the dentate nucleus specifically, and the mesencephalon rather than the thalamus, it is perhaps possible that the identified tract is not actually the DTT. We believe this is unlikely, given that the dentate nucleus and red nucleus were manually contoured whereas the ventrolateral thalamus was localized with stereotactic coordinates, and given that all 3 structures were consistently involved in the tract that we called the DTT. Nevertheless, to confirm, we are currently investigating the tract with the

aid of more advanced imaging software, which will use the dentate and the ventrolateral thalamus directly as the ROIs.

Conclusions

Using diffusion-weighted MRI sequences and diffusion tensor tractography, we identified in humans both of the tracts described in primates that connect the cerebellum and basal ganglia, confirming the existence of independent circuitry between the basal ganglia and cerebellum. In patients with PD undergoing DBS, the electrode contact that produced clinical benefit was found to be in proximity to the DTT within the VTA, suggesting a possible benefit with stimulation of this target. These findings lend support to the notion that the tracts may be stimulated by DBS therapy and that improved targeting may eventually lead to better outcomes.

References

1. Amtage F, Henschel K, Schelter B, Vesper J, Timmer J, Lucking CH, et al. Tremor-correlated neuronal activity in the subthalamic nucleus of Parkinsonian patients. Neurosci Lett. 2008; 442:195–199. [PubMed: 18634849]
2. Bostan AC, Dum RP, Strick PL. The basal ganglia communicate with the cerebellum. Proc Natl Acad Sci USA. 2010; 107:8452–8456. [PubMed: 20404184]
3. Bostan AC, Strick PL. The cerebellum and basal ganglia are interconnected. Neuropsychol Rev. 2010; 20:261–270. [PubMed: 20811947]
4. Butson CR, Cooper SE, Henderson JM, Mclntyre CC. Patient-specific analysis of the volume of tissue activated during deep brain stimulation. Neuroimage. 2007; 34:661–670. [PubMed: 17113789]
5. Coenen VA, Mädler B, Schiffbauer H, Urbach H, Allert N. Individual fiber anatomy of the subthalamic region revealed with diffusion tensor imaging: a concept to identify the deep brain stimulation target for tremor suppression. Neurosurgery. 2011; 68:1069–1076. [PubMed: 21242831]
6. Defer GL, Widner H, Marie RM, Remy P, Levivier M. Core assessment program for surgical interventional therapies in Parkinson's disease (CAPSIT-PD). Mov Disord. 1999; 14:572–584. [PubMed: 10435493]
7. Fishman PS. Paradoxical aspects of parkinsonian tremor. Mov Disord. 2008; 23:168–173. [PubMed: 17973325]
8. Follett KA, Weaver FM, Stern M, Hur K, Harris CL, Luo P, et al. Pallidal versus subthalamic deep-brain stimulation for Parkinson's disease. N Engl J Med. 2010; 362:2077–2091. [PubMed: 20519680]
9. Grafton ST, Turner RS, Desmurget M. Normalizing motor-related brain activity: subthalamic nucleus stimulation in Parkinson disease. Neurology. 2006; 66:1192–1199. [PubMed: 16636237]
10. Guridi J, Rodriguez-Oroz MC, Arbizu J, Alegre M, Prieto E, Landecho I, et al. Successful thalamic deep brain stimulation for orthostatic tremor. Mov Disord. 2008; 23:1808–1811. [PubMed: 18671286]
11. Hamel W, Fietzek U, Morsnowski A, Schrader B, Herzog J, Weinert D, et al. Deep brain stimulation of the subthalamic nucleus in Parkinson's disease: evaluation of active electrode contacts. J Neurol Neurosurg Psychiatry. 2003; 74:1036–1046. [PubMed: 12876231]
12. Hoshi E, Tremblay L, Féger J, Carras PL, Strick PL. The cerebellum communicates with the basal ganglia. Nat Neurosci. 2005; 8:1491–1493. [PubMed: 16205719]
13. Hurtado JM, Gray CM, Tamas LB, Sigvardt KA. Dynamics of tremor-related oscillations in the human globus pallidus: a single case study. Proc Natl Acad Sci U S A. 1999; 96:1674–1679. [PubMed: 9990083]
14. Kelly RM, Strick PL. Cerebellar loops with motor cortex and prefrontal cortex of a nonhuman primate. J Neurosci. 2003; 23:8432–8444. [PubMed: 12968006]

15. Lenz FA, Tasker RR, Kwan HC, Schnider S. Single unit analysis of the human ventral thalamic nuclear group: correlation of thalamic tremor cells with the 3-6 Hz component of parkinsonian tremor. J Neurosci. 1988; 8:754–764. [PubMed: 3346719]
16. Limousin P, Krack P, Pollak P, Benazzouz A, Ardouin C, Hoffmann D, et al. Electrical stimulation of the subthalamic nucleus in advanced Parkinson's disease. N Engl J Med. 1998; 339:1105–1111. [PubMed: 9770557]
17. Miocinovic S, Parent M, Butson CR, Hahn PJ, Russo GS, Vi-tek JL, et al. Computational analysis of subthalamic nucleus and lenticular fasciculus activation during therapeutic deep brain stimulation. J Neurophysiol. 2006; 96:1569–1580. [PubMed: 16738214]
18. Ostrem, JL. Patient selection: when to consider deep brain stimulation for patients with Parkinson's disease, essential tremor, or dystonia. In: Marks, W., editor. Deep Brain Stimulation Management. Cambridge: Cambridge University Press; 2011. p. 4-19.
19. Percheron G, Francois C, Talbi B, Yelnik J, Fenelon G. The primate motor thalamus. Brain Res Brain Res Rev. 1996; 22:93–181. [PubMed: 8883918]
20. Plaha P, Ben-Shlomo Y, Patel NK, Gill SS. Stimulation of the caudal zona incerta is superior to stimulation of the subthalamic nucleus in improving contralateral parkinsonism. Brain. 2006; 129:1732–1747. [PubMed: 16720681]
21. Rascol O, Sabatini U, Fabre N, Brefel C, Loubinoux I, Celsis P, et al. The ipsilateral cerebellar hemisphere is overactive during hand movements in akinetic parkinsonian patients. Brain. 1997; 120:103–110. [PubMed: 9055801]
22. Walter BL, Vitek JL. Surgical treatment for Parkinson's disease. Lancet Neurol. 2004; 3:719–728. [PubMed: 15556804]
23. Wu T, Hallett M. A functional MRI study of automatic movements in patients with Parkinson's disease. Brain. 2005; 128:2250–2259. [PubMed: 15958505]
24. Yu H, Sternad D, Corcos DM, Vaillancourt DE. Role of hyperactive cerebellum and motor cortex in Parkinson's disease. Neuroimage. 2007; 35:222–233. [PubMed: 17223579]

Abbreviations used in this paper

DBS	deep brain stimulation
DTT	dentatothalamic tract
DWI	diffusion-weighted imaging
PD	Parkinson disease
ROI	region of interest
SPCT	subthalamopontocerebellar tract
STN	subthalamic nucleus
UPDRS	Unified Parkinson's Disease Rating Scale
VTA	volume of tissue activated

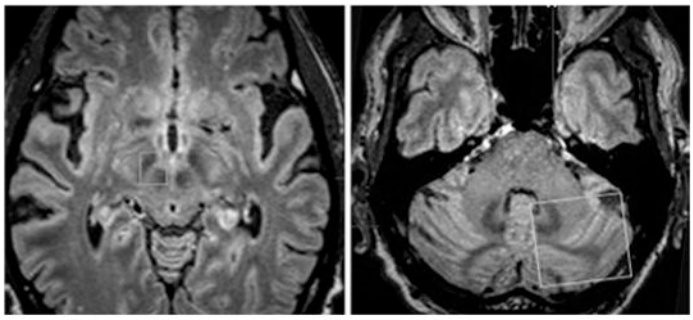

FIG. 1.

To identify the tracts, 2 ROIs were defined on MRI FLAIR sequences, one overlying the right STN and the red nucleus **(left)** and the other overlying the contralateral cerebellar hemisphere **(right)**.

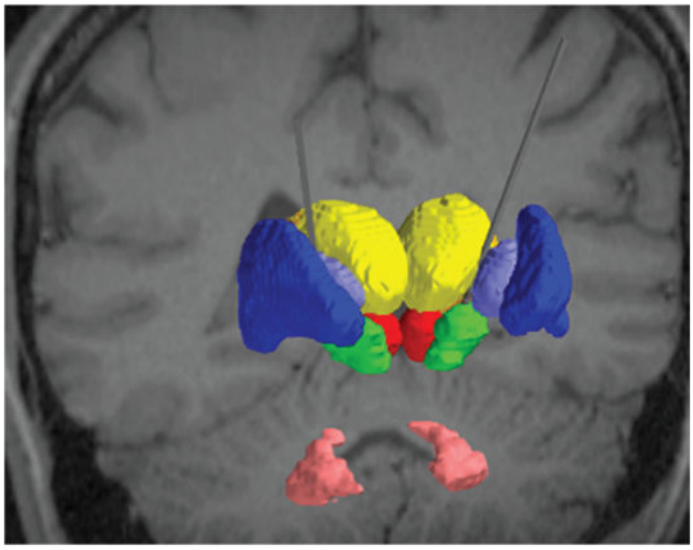

FIG. 2.

For the subset of individuals who underwent DBS of the STN, we created patient-specific computer models of DBS. Each model integrated into a common platform the patient imaging data, 3D subcortical nuclei, DBS electrode, and the VTA. The relevant nuclei were contoured and include the globus pallidus and putamen *(blue)*, the thalami *(yellow)*, the red nuclei *(red)*, the STN *(green)*, and the dentate nuclei *(pink)*.

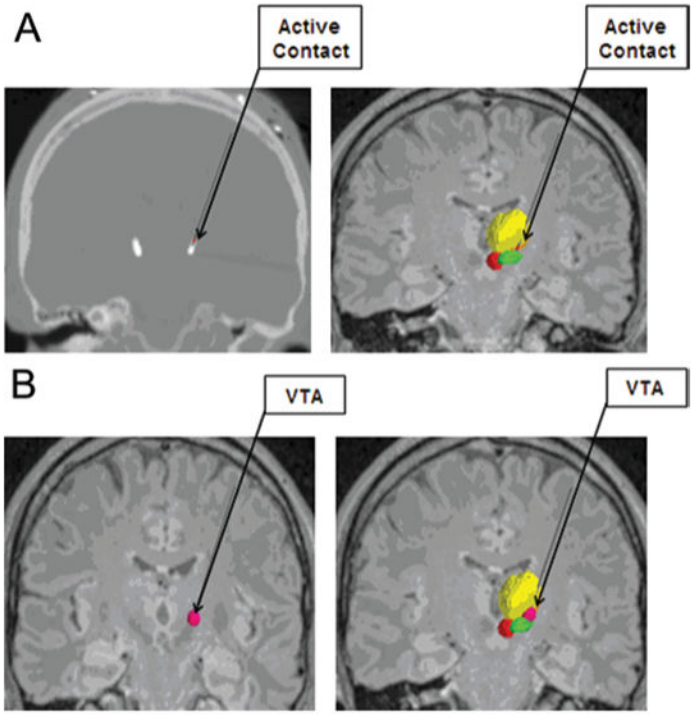

FIG. 3.

A: The active contact of each electrode was determined from postoperative programming sessions, and was defined as the cathodal electrode for either monopolar or bipolar stimulation. The active contact is shown on a postoperative CT scan **(left)** and on image fusion on MRI **(right)**. **B**: The VTA was calculated from each patient's specific stimulation parameter settings by using a custom Python-based program from Python libraries. The VTA is shown in *dark pink* alone **(left)** and in conjunction with the contoured nuclei **(right)**.

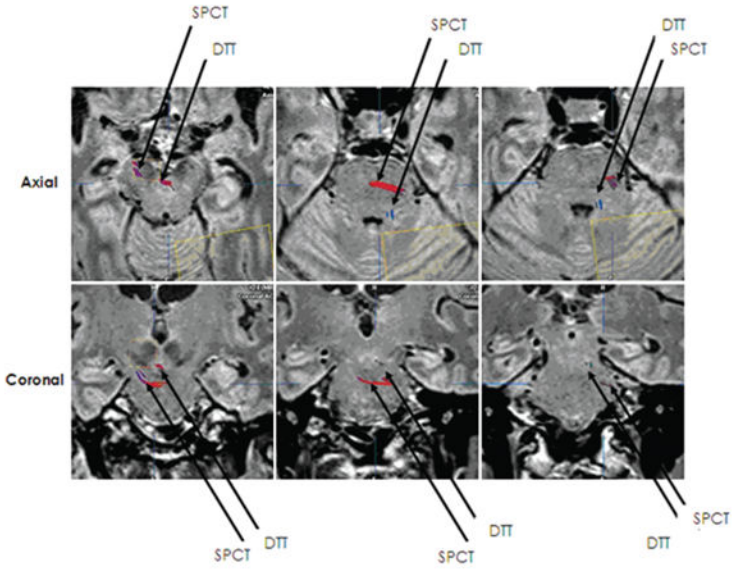

FIG. 4.

Two distinct tracts were identified, corresponding to the previously described course of the SPCT and the DTT.

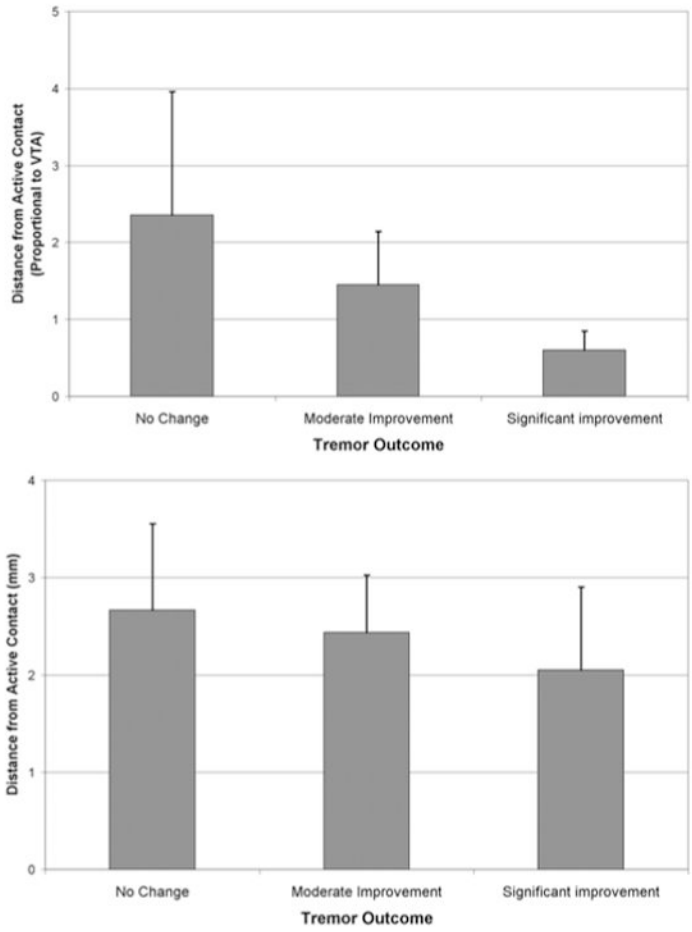

FIG. 5.

Bar graphs showing outcomes according to electrode position. **Upper**: There was a nonsignificant trend toward better outcome when the active contact was closer to the DTT. **Lower**: There was a greater trend toward correlation with outcome when the distance proportional to VTA rather than actual distance was considered.

TABLE 1

Demographic data and presenting symptoms in 14 patients with PD*

Case No.	Age (yrs), Sex	Hand	Sxs	Side of > Sxs	Side of > Tremor	Side of Electrode	Off	On	% Imp
1	69, M	lt	T>B>R	rt	rt	lt	35	25	28.6
2	66, M	rt	T>R>B	rt	equal	bilat	41	24	41.5
3	55, F	rt	B>R	lt	NA	bilat	27	11.5	57.4
4	49, M	rt	T>R>B	lt	lt	rt	26	10.5	59.6
5	74, M	rt	R>B	lt	NA	bilat	41	19	53.7
6	62, F	rt	T>R>B	lt	equal	bilat	34	12	64.7
7	63, F	lt	B>R>T	lt	NA	bilat	54	33.5	38.0
8	64, F	rt	B>T>R	rt	rt	bilat	32	12	62.5
9	64, M	rt	R>T>B	lt	lt	bilat	26.5	14.5	45.3
10	56, F	rt	T>R>B	rt	rt	NA	32	14	56.3
11	72, F	rt	R>B>T	rt	rt	NA	58	49.5	14.7
12	76, M	lt	B>R	lt	NA	NA	27.5	18.5	32.3
13	78, M	rt	R>B>T	lt	lt	NA	33	16	51.5
14	56, M	rt	B>R>T	rt	rt	NA	31	16.5	46.8

*B = bradykinesia; Imp = improvement; NA = not applicable; R = rigidity; Sx = symptom; T = tremor.

TABLE 2

Programming settings and benefits in 9 patients with PD treated with DBS*

Case No.	Cathode	Anode	Amplitude (V)	Pulse Width (msec)	Frequency (Hz)
1	It: 3	It: C	It: 3	It: 90	It: 180
2	It: 1, rt: 2	It: C, rt: C	It: 3, rt: 3	It: 60, rt: 60	It: 130, rt: 130
3	It: 2, rt: 2	It: C, rt: 3	It: 2.5, rt: 3	It: 60, rt: 60	It: 130, rt: 130
4	rt: 1	It: C	rt: 2.4	rt: 60	rt: 130
5	It: 2, rt: 0	It: C, rt: 2	It: 2, rt: 1.8	It: 60, rt: 60	It: 130, rt: 130
6	It: 0, rt: 1	It: C, rt: C	It: 2, rt: 2.5	It: 60, rt: 60	It: 130, rt: 130
7	It: 2, rt: 3	It: C, rt: 1	It: 3.2, rt: 3.5	It: 60, rt: 60	It: 130, rt: 130
8	It: 2, rt: 2	It: C, rt: C	It: 2, rt: 2	It: 60, rt: 60	It: 130, rt: 130
9	It: 2, rt: 2	It: C, rt: C	It: 2, rt: 2	It: 60, rt: 60	It: 130, rt: 130

*All patients experienced a benefit from DBS. C = case.

TABLE 3

Location of active contact relative to midcommissural point in 9 patients with PD treated with DBS*

Case No.	Coordinate (mm)					
	Rt Lat	Rt Pst	Rt Inf	Lt Lat	Lt Pst	Lt Inf
1				12.22	2.83	0.94
2	12.63	3.95	3.25	12.32	2.29	4.20
3	14.85	2.28	0.49	11.22	0.95	1.20
4	14.26	2.84	1.97	NA	NA	NA
5	11.01	5.49	5.98	12.55	3.68	1.42
6	9.90	2.25	4.73	8.55	5.23	7.62
7	13.16	2.76	0.09	12.15	3.62	0.85
8	12.32	1.67	1.21	11.50	0.66	2.07
9	13.87	2.12	2.96	14.26	1.07	2.97

* Inf = inferior; pst = posterior.

J Neurosurg. Author manuscript; available in PMC 2016 January 11.

TABLE 4

Tremor, bradykinesia, and rigidity subscores in 9 patients with PD treated with DBS*

Case No.	Sxs	Side of Electrode	Preop Score	Postop Score
tremor				
1	T>B>R	It	rt: 4, It: 2.5, M: 1, T: 2.5	rt: 4, It: 3, M: 0, T: 2.33
2	T>R>B	bilat	rt: 6, It: 6, M: 1, T: 4.33	rt: 1, It: 0.5, M: 0, T: 0.5
3	B>R	bilat	rt: 0, It: 0, M: 0, T: 0	rt: 1, It: 1.5, M: 0, T: 0.83
4	T>R>B	rt	rt: 3, It: 8.5, M: 0, T: 3.83	rt: 2, It: 6, M: 0, T: 2.67
5	R>B	bilat	rt: 0, It: 0, M: 0, T: 0	rt: 0, It: 0, M: 0, T: 0
6	T>R>B	bilat	rt: 3, It: 3, M: 2, T: 2.67	rt: 1, It: 1, M: 1, T: 1
7	B>R>T	bilat	rt: 1, It: 1, M: 1, T: 1	rt: 0, It: 0, M: 0, T: 0
8	B>T>R	bilat	rt: 4, It: 0, M: 2, T: 2	rt: 0, It: 0, M: 0, T: 0
9	R>T>B	bilat	rt: 2, It: 3, M: 0.5, T: 1.83	rt: 1, It: 3, M: 0, T: 1.3
bradykinesia				
1	T>B>R	It	rt: 4, It: 3, M:2, T: 2.25	rt: 4, It: 4, M: 1, T.2.25
2	T>R>B	bilat	rt: 4, It: 3, M: 2, T: 2.25	rt: 1.5, It: 1, M: 0.5, T: 0.75
3	B>R	bilat	rt: 2, It: 3, M: 4.5, T: 2.38	rt: 3, It: 4, M:5, T:4
4	T>R>B	rt	rt: 1, It: 3, M: 0.5, T: 1.13	rt: 3, It: 6, M: 2, T: 2.75
5	R>B	bilat	rt: 3, It: 3.5, M: 4.5, T: 2.75	rt: 2, It: 3.5, M: 2, T: 1.88
6	T>R>B	bilat	rt: 2, It: 3.5, M: 3.5, T: 2.25	rt: 2, It: 2, M: 1.5, T: 1.38
7	B>R>T	bilat	rt: 6, It: 5, M: 7, T: 4.5	rt: 3, It: 5, M: 4, T: 3
8	B>T>R	bilat	rt: 3.5, It: 1.5, M: 4, T: 2.25	rt: 1, It: 1, M: 1, T: 0.75
9	R>T>B	bilat	rt: 0.5, It: 2, M: 2, T: 1.13	rt: 1, It: 2, M: 0, T: 0.75
rigidity				
1	T>B>R	It	rt: 2, It: 2, M: 2, T: 2	rt: 2, It: 1, M: 2, T: 1.67
2	T>R>B	bilat	rt:4, It: 3, M: 1, T: 2.67	rt: 0, It: 0, M: 1, T: 0.33
3	B>R	bilat	rt: 1, It: 1, M: 0, T: 0.67	rt: 2, It: 3, M: 1, T: 2
4	T>R>B	rt	rt: 2, It: 3, M: 1, T: 2	rt: 1, It: 2, M: 1, T: 1.33
5	R>B	bilat	rt: 4.5, It: 4.5, M: 2.5, T: 3.83	rt: 1.5, It: 2, M: 1, T: 1.5
6	T>R>B	bilat	rt: 2, lt:4, M: 1, T: 2.33	rt: 0.5, It: 0.5, M: 2, T: 1.3
7	B>R>T	bilat	rt: 3.5, It: 4, M: 3, T: 3.5	rt: 1, It: 1, M: 2.5, T: 1.5
8	B>T>R	bilat	rt: 2, It: 2, M: 1, T: 1.67	rt: 0, It: 1, M: 1, T: 0.67
9	R>T>B	bilat	rt: 3, It: 4, M:1, T:2.67	rt: 0, It: 1, M: 0, T: 0.33

* See “Clinical Data Collection” for scoring method. M = midline.